Hollow structure in nanosecond pulsed pin-pin discharge during the breakdown phase

C. Chen[1,2,3], M. Simeni Simeni[1], S. Li[2,3] and P.J. Bruggeman[1]

[1]*Department of Mechanical Engineering, University of Minnesota, Minneapolis, USA*
[2]*Key Laboratory of Material Modification by Laser, Ion, Electron Beams, Dalian University of Technology, Dalian, People's Republic of China*
[3]*School of Physics, Dalian University of Technology, Dalian, People's Republic of China*

Abstract: In this work we report the observation of a hollow structure in atmospheric pressure nanosecond pulsed pin-pin discharges. This effect is observed at the initial stage of the discharge formation. Previously such phenomenon has been observed in pinched plasmas. The phenomenon is investigated in detail in pure helium discharges and an explanation of the phenomenon based on electron quenching of the excited states due to the high electric field strength is proposed.

Keywords: nanosecond pulse discharge, hollow structure, breakdown phase, electric field.

1. Introduction

Over the last decade, there has been a huge increase in studies of repetitively nanosecond pulsed discharges. These discharges have properties that can be exploited in multiple applications such as combustion [1-3], material processing [4], plasma medicine [5] and gas treatment [6-8] to name a few. Nonetheless many unknowns remain regarding fundamental kinetic mechanisms of these discharges. This includes breakdown and fast ionization mechanisms, fast gas heating in gases other than air and the generation of exceptionally large electron densities. Discharges generated by nanosecond voltage pulses with fast nanosecond and sub-nanosecond rise times are known to generate more homogeneous breakdown.

We focus in this study on nanosecond pulsed discharges in atmospheric pressure helium generated in a pin-pin electrode geometry. We report on the dynamics during the breakdown phase.

2. Experimental Setup

Figure 1 shows a schematic of the experimental setup. The discharge is produced between two tungsten pin electrodes separated by a gap distance of about 4.2 mm. The upper and bottom electrode are circular cylinders with diameters of 1 and 3.3 mm respectively and have tapered tips with a radius of ~ 0.15 mm. The chamber is pumped down and filled three times with helium before the start of the experiment. The flow rate is kept constant at 1 L/min. The gas outlet is controlled by an over-pressure valve in order to maintain the pressure of the chamber constant at 1 atm. The nanosecond pulsed helium discharge (see the inset in Fig. 1) is the focus of this work because it is more diffuse and stable compared to similar discharges in other gases. In addition it requires a relatively low voltage to generated reproducible discharges.

High voltage pulses with an amplitude of 3 to 6 kV, duration of 200 ns and a 1kHz repetition rate were generated by a DEI PVX-4110 high voltage pulse generator. A resistor of R = 1 kΩ was placed between the bottom pin and the ground to limit the current.

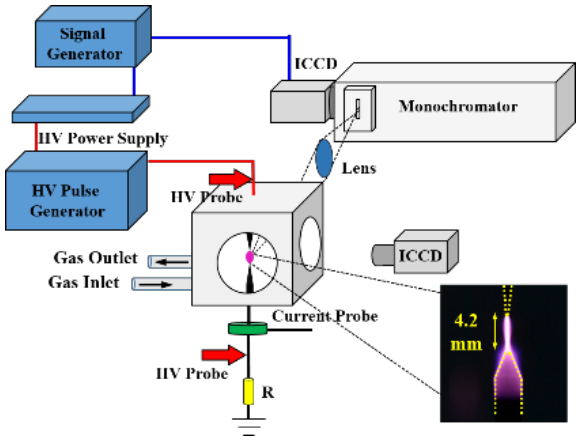

Fig. 1. Schematic diagram of the experimental setup.

A Spellman SL150 DC power supply was employed to deliver high-voltage to the high voltage pulse generator. The discharge voltage was measured using two high voltage probes (Tektronix P6015A, 75 MHz bandwidth) as indicated in Fig. 1 and the current was measured by a Rogowski coil (Pearson 6585, 200 MHz bandwidth) placed between the bottom pin and the resistor. The current and voltage waveforms were recorded by a digital oscilloscope (Rigol DS1204B, 1GS/s). By measuring the current on the low voltage side we only recorded the conduction current. The maximum energy coupled to the plasma was about 500 μJ/pulse (for the 6 kV case).

The discharge was investigated using intensified CCD plasma imaging and optical emission spectroscopy. The discharge dynamics were studied by recording time resolved single-shot plasma images using an Andor iStar DH340T ICCD camera with a UV lens (Nikkor, 105 mm, *f*/4.5). The minimum exposure time of the camera is 3 ns.

The ICCD was externally triggered by a TTL output signal from the same function generator also used to trigger the high voltage pulse generator.

Optical emission spectroscopy was used to determine the gas temperature, electron density and electric field measurements during the early stages of the discharge. A UV-NIR achromatic triple lens (f = 90 mm) was used in a 2f-2f configuration to image the plasma filament on the entrance slit of an Acton Research Corporation monochromator (AM510, f = 1000 mm) equipped with a 1800 grooves/mm grating. During the experiments, the entrance slit width was fixed at 50 µm resulting in a spectral resolution of ~ 50 pm. All the spectroscopic measurements were performed in the middle of the discharge gap.

The gas temperature was inferred from the rotational temperature of the N_2(C-B) (0-0) transition, present due to the nitrogen impurities in the chamber [9-10].

The electron densities were determined from the Stark broadening of the helium I line at 492.2 nm [11-12]. This method was first validated comparing its results with the electron density obtained from H_β Stark broadening in a humid helium discharge.

The electric field was measured through the study of the Stark effect-induced splitting and shifting of the same He I line at 492.2 nm [13-16]. This required adding a polarizer plate in front of the entrance slit of the monochromator. The polarizer was oriented such that it only transmits the vertical component of the electric field, parallel to the axis of symmetry of the discharge. A 5 ns camera gate was employed and each recorded spectrum consists of 10,000 accumulations.

3. Results and discussion

Figure 2 shows the temporal evolution of discharges in helium for four different applied voltages. At 3 kV the discharge column is readily apparent between the two pins and its emission intensity increases gradually as the conductive current increases. The discharge right after breakdown evolves as a cathode-directed streamer, which is not temporally resolved here. When the applied voltage increases from 4 to 5 kV or higher, a hollow structure in light emission appears that precedes the formation of the spark discharge. In addition, the size of the hollow region and the discharge channel width increases with increasing voltage amplitude. This suggests that the appearance of the hollow structure depends on the applied voltage with the threshold voltage being around 4 kV.. The observation of an increase in discharge radius is consistent with the previously reported increase in thickness of streamers for high over-voltages in air [17] and suggests that the discharge is generated at over-voltages in He for 4 to 6 kV.

The hollow profiles were observed in different gases (data not shown) suggesting that the formation of the hollow structure is not strongly gas dependent.

The electric field in the centre of the gap at the initial stage of the discharge in helium is measured by the intensity ratio of the π-components of the allowed and forbidden components of the 492.2 nm line. The determination of the electric field was only feasible during the onset of the discharge when the electron density is sufficiently low not to broaden the forbidden and allowed component and hence make them indistinguishable from each other. The inferred electric field strengths displayed in Fig. 3 for applied voltages of 3 and 5 kV are 5.8 ± 0.4 and 8.2 ± 0.2 kV/cm at the first visible emission. However the DC breakdown voltage of helium at atmospheric pressure given by the Paschen's law is only about 4 kV/cm, which is consistent with a breakdown at over-voltage.

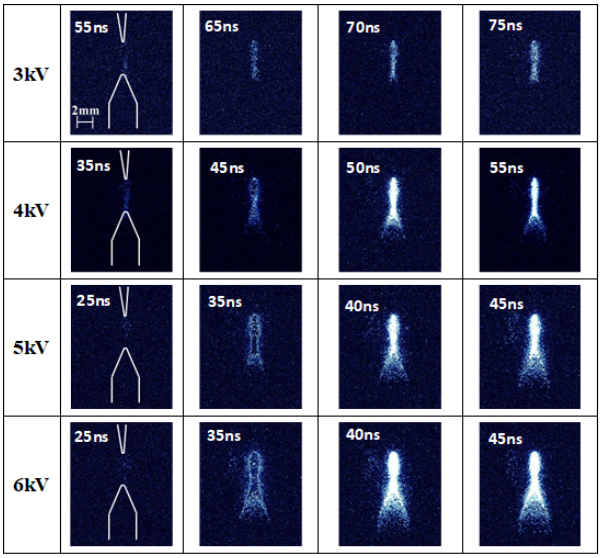

Fig. 2. Time-resolved single-shot ICCD images of the helium discharge. The gate width is 5 ns.

As a result, the appearance of the hollow structure seems to be correlated with high electric fields since the overvoltage leads to an increase of the breakdown field when the applied voltage amplitude is increased. Because the hollow structure in the emission intensity occurs at the initial stage of the discharge, a first order approximation of the maximum electric field can be made by the Laplacian electric field. As expected, the Laplacian electric field in the middle of the electric gap exceeds the measured electric field values due to the presence of space charge. The reduced electric field, obtained from the Laplacian electric field, at which the hollow structure in the emission profile appears is approximately 30 Td.

We propose a mechanism involving the depopulation of radiative states by energetic electrons in these high electric field to explain the hollow profile. Indeed, estimates of the electron-induced excitation frequencies of radiative excited states responsible for the observed emission start to become significantly larger than the Einstein coefficients of the excited states for the experimental conditions at which the hollow emission profile is found.

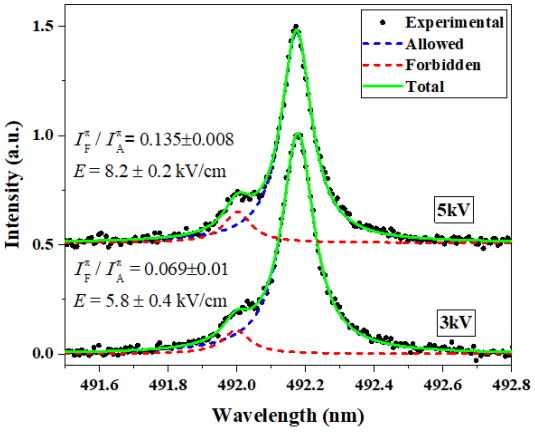

Fig. 3. π-polarized emission spectra of the allowed ($1s2p$ $^1P_1$-$1s4d$ $^1D_2$) and forbidden ($1s2p$ $^1P_1$-$1s4f$ $^1F_3$) components of the He I 492 nm lines. The applied voltage of the discharge is 3 and 5 kV obtained at the first visible emission.

4. Conclusions

Hollow structures in pin-pin nanosecond pulsed discharges in atmospheric pressure helium have been observed during the breakdown phase using time-resolved ICCD imaging. The hollow profiles have been observed in different gases hence suggesting that their cause is in first approximation gas independent. The detailed study of discharges in helium showed that the phenomenon can be controlled by increasing the applied voltage amplitude, exhibiting a threshold at 4 kV in our studies. Electric field measurements carried out at the early stages of the discharge feature fields much higher than 4 kV/cm, which is the DC breakdown field of helium at atmospheric pressure. The results suggest that in these discharges, at the initial high electric field, electron-induced depopulation of radiative states via excitation causes the formation of the hollow structure in the emission profile.

5. Acknowledgments

The authors would like to acknowledge funding provided by the Department of Energy, Office of Fusion Energy Science grant through the general Plasma Science Program (AT4010100) and the University of Minnesota. Chuan-Jie Chen acknowledges the Chinese Scholarship Council for his fellowship (No. 201706060142) to support his research stay at the University of Minnesota.

6. References

[1] G. Pilla et al, IEEE Transactions on Plasma Science, 34 (6) 2471-2477 (2006)
[2] S. Starikovskaia et al., 43rd Aerospace Science Meeting and Exhibit (2005)
[3] N. Popov, J. Phys. D: Appl. Phys., 44, 285201 (2011)
[4] D. Pai, J. Phys. D : Appl. Phys., 44, 174024 (2011)
[5] G. Fridman et al, Plasma Process and Polymers 5 (6) 503-533 (2008)
[6] E.M. Veldhuizen et al., Plasma Chem. Plasma Process. 16 (2) 227-247 (1996)
[7] R. Ono and T. Oda, J. Phys. D: Appl. Phys., 40, 176-182 (2007)
[8] N. Blin-Simian et al, Plasma Process Polym. 2 (3) 256-262 (2005)
[9] Q. Wang et al, J. Phys D: Appl. Phys., 40 (14) 4202-4211 (2007)
[10] P.J. Bruggeman et al, Plasma Sources Sci. Technol., 23, 023001 (2014)
[11] N. Lara et al, Astron. Astrophys., 542, A75 (2012)
[12] S. Yatom et al, Phys. Rev. E, 88, 013107 (2013)
[13] J.S. Foster and N. Bohr, Royal Soc. Proc., 117 (776) 137-163 (1927)
[15] P. Olszewski et al, Plasma Sources Sci. Technol., 23, 015010 (2014)
[16] P.M. Obradovic and M.M. Kuraica, Phys. Lett. A. 372.(2) 137-140 (2008)
[17] T.M.P. Briels et al, J. Phys, D : Appl. Phys., 41, 234008 (2008)